Atmos. Sci. Lett. (2014)
Published online in Wiley Online Library
(wileyonlinelibrary.com) **DOI:** 10.1002/asl2.552

RMetS
Royal Meteorological Society

Pathways between soil moisture and precipitation in southeastern South America

Romina C. Ruscica,[1]* Anna A. Sörensson[1] and Claudio G. Menéndez[1,2]
[1]*Centro de Investigaciones del Mar y la Atmósfera, CONICET/UBA, UMI IFAECI/CNRS, Buenos Aires, Argentina*
[2]*Departamento de Ciencias de la Atmósfera y los Océanos, FCEN, UBA, Buenos Aires, Argentina*

**Correspondence to:*
R. C. Ruscica, CIMA (CONICET-UBA), Ciudad Universitaria, Int. Guiraldes 2160, Pabellón 2, Piso 2, Ciudad Autónoma de Buenos Aires C1428EGA, Argentina.
E-mail: ruscica@cima.fcen.uba.ar

Received: 29 May 2014
Revised: 10 November 2014
Accepted: 12 November 2014

Abstract

Southeastern South America (SESA) is found to be the main hot spot of soil moisture–evapotranspiration coupling of South America during a dry summer. However, only its eastern part is a soil moisture–precipitation hot spot. Pathways between soil moisture and precipitation are evaluated through studying the coupling of soil moisture with surface and boundary layer variables. The outcome suggests that both the moist static energy and its vertical gradient are important for the development of precipitation, as a result of the total surface heat fluxes that are affected by soil moisture only in the eastern part of SESA.

Keywords: soil moisture; precipitation; coupling strength; southeastern South America; moist static energy; regional climate modelling

1. Introduction

Land–atmosphere interactions over southeastern South America (SESA) have been recognized as an important issue for a correct representation of regional climate during the austral summer season. A major improvement in the simulated low-level winds, sensible heat flux and Bowen ratio (BR) was achieved when both soil and vegetation processes were included in a land surface scheme coupled to a climate model (Ma *et al.*, 2011). Surface temperature and precipitation were better represented when soil moisture–atmosphere interactions were taken into account (Barreiro and Díaz, 2011). SESA has also been identified as a hot spot region, where both soil moisture – evapotranspiration and soil moisture – precipitation coupling are strong (Sörensson and Menéndez, 2011). The concept of coupling refers to the influence of soil moisture on some variable, isolating it from the reverse influence of the variable on soil moisture. In particular, this is important when studying precipitation, which exerts a strong control on soil moisture. Ruscica *et al.* (2014) found that the deep soil moisture memory is lower inside the soil moisture – evapotranspiration hot spot in SESA, than in other regions of southern South America, i.e. the soil moisture memory and the strength of the coupling are anticorrelated within the hot spot.

The coupling strength (CS) index permits isolating and quantifying how much the soil moisture influences on the atmosphere using a methodology based on model experiments (Koster *et al.*, 2004). Coupling strength studies have diagnosed the coupling between soil moisture and precipitation (e.g. Koster *et al.*, 2006), evapotranspiration (e.g. Guo *et al.*, 2006), 2 m temperature (e.g. Seneviratne *et al.*, 2006) and surface sensible and latent heat fluxes (e.g. Guo and Dirmeyer, 2013). The coupling between soil moisture and precipitation tends to be less robust than the coupling between other variables because there are many processes that influence precipitation ranging from local to regional to large scale. It is therefore important to assess the different variables that connect soil moisture to precipitation. Analysis range from the simplest 'soil moisture–evapotranspiration-precipitation chain' (e.g. Sörensson and Menéndez, 2011; Wei and Dirmeyer, 2012) to more complex systems which can include several pathways (e.g. Santanello *et al.*, 2011).

This study is designed with two purposes: first to determine whether the SESA region is a hot spot of soil moisture and precipitation coupling during anomalously dry and wet soil moisture conditions for different seasons of the year, and second to study the processes involved in creating favourable conditions for high soil moisture–precipitation coupling strength.

2. Model and methodology

In order to study the coupling index we follow an approach similar to Koster et al. (2006), which require performing ensembles of simulations with a climate model. The Rossby Centre Atmospheric regional model (RCA4, Samuelsson *et al.*, 2011) is used for this study. This model has been used for climate studies in South America in the context of the CLARIS and CLARIS LPB projects (http://www.claris-eu.org/, Menéndez *et al.*, 2010; Solman *et al.*, 2013). The geographical domain covers South America with a horizontal resolution of 0.44° and 40 vertical levels. ERA-Interim reanalysis data are used at 0.75° horizontal resolution for the

initial and boundary conditions (Dee *et al.*, 2011). For soil moisture (SM) prognostic variables, the soil column is divided into three layers where the two upper layers have a depth of 7 and 21 cm respectively, and the depth of the lowest layer is defined from the rooting depth of the Ecoclimap database (Masson *et al.*, 2003). RCA4 employs three land surface cover tiles for the separate calculation of fluxes of momentum and latent and sensible heat fluxes: open land, coniferous forest and broadleaved forest. The open land tile is subdivided into a vegetated and a bare soil part, and the two forest tiles include the canopy and the forest floor. The vegetation and soil parameters are taken from Ecoclimap.

A favourable condition for soil moisture to induce a response in precipitation (PP) is that the evapotranspiration (ET) variability is high (Guo *et al.*, 2006). As this condition is not met in SESA during austral winter (JJA), the study focuses on spring (SON), summer (DJF) and autumn (MAM). For each one of these seasons, one dry and one wet year from a simulation spanning 1980–1999, are identified through examining the seasonal soil water availability anomaly for a rectangle identified over the SESA region (see Figure 1). The dry periods selected are SON of 1988, DJF of 1988–1989 and MAM of 1989 and the wet periods are SON of 1985, DJF of 1997–1998 and MAM of 1998. For each of these six cases, the seasonal coupling strength index CS is calculated.

The methodology consists in the comparison of a similarity index (Ω) for two ensembles, one with prescribed soil moisture conditions (ensemble S) and the other with free interaction between surface and atmosphere (ensemble W). Each ensemble consists of 15 members, which were initialized on different dates so that each simulation has at least 45 days of atmospheric spin up. In order to have the soil in equilibrium with the atmosphere, the soil moisture initial conditions were taken from a multi-year integration so that each simulation has at least 2 years of soil moisture spin up. The Ω_X index measures the similarity of the amplitude, phase and mean of ensemble members of variable X (Yamada *et al.*, 2007), and quantifies the signal variance respect to the total variance (signal + noise) through the equation:

$$\Omega_X = \frac{15\,\sigma^2_{\hat{X}} - \sigma^2_X}{14\,\sigma^2_X} \tag{1}$$

where $\sigma^2_{\hat{X}}$ is the variance of the mean time series of all members of the ensemble and σ^2_X is the ensemble inter member variance which was obtained by calculating the variance among all time steps and ensemble members. The synoptic scale was filtered by using time series of 6-day mean values. Then, the coupling strength of the variable X (hereafter CS[SM,X]) is calculated as the difference between the Ω_X of the ensembles:

$$\mathrm{CS[SM},X] = \Omega_X\,(\mathrm{S}) - \Omega_X\,(\mathrm{W}) \tag{2}$$

As soil moisture is a boundary condition only for the ensemble S, CS[SM,X] is positive over regions where soil moisture explains some of the variance of X. In the following, coupling strength of different variables that connect soil moisture with precipitation is analysed.

3. Results

High values of both the coupling strength of evapotranspiration (CS[SM,ET]) and its daily variability (σ_{ET}) have been proposed to be necessary conditions for soil moisture to have a controlling effect over precipitation (Guo *et al.*, 2006). To identify when this occurs for the six cases, the product of these two statistics $\mathrm{CS[SM,ET]} \times \sigma_{\mathrm{ET}}$ (defined by Ruscica *et al.* (2014) as the 'coupling efficiency') is shown over South America in Figure 1. In general, the $\mathrm{CS[SM,ET]} \times \sigma_{\mathrm{ET}}$ hot spots appear over SESA and neighbouring regions and over the eastern coast of Brazil. Over the SESA region, CS[SM,ET] is higher for dry conditions than for wet conditions while the σ_{ET} is highest over SESA in DJF (not shown). The strongest coupling efficiency occurs when the land surface is dry during DJF (Figure 1(e)). Figure 2 shows that the coupling strength of precipitation (CS[SM,PP]) is weaker and less spatially coherent than $\mathrm{CS[SM,ET]} \times \sigma_{\mathrm{ET}}$, and that during the dry DJF the eastern SESA region is one of the main CS[SM,PP] hot spots while northwestern SESA has a CS[SM,PP] close to zero. In the following, we will therefore focus on the dry DJF season to understand why soil moisture controls precipitation only in the eastern SESA although the coupling efficiency is high over the entire region.

Eltahir (1998) proposed a theory of pathways between soil moisture conditions and subsequent rainfall, based mainly on considerations of the energy balance, in order to dissect the soil moisture influence on precipitation. To study the processes leading to high CS[SM,PP] in eastern SESA, some of these pathways were examined by analysing the coupling strength between soil moisture and the variables in Figure 3.

Most of the total energy in the boundary layer can be described by the moist static energy (MSE):

$$\mathrm{MSE} = c_{\mathrm{p}}T + Lq + gZ \tag{3}$$

where the terms on the right hand side represent the internal, latent and potential energies (with c_{p} the specific heat of dry air at constant pressure, T the air temperature, L the latent heat of vaporization, q the specific humidity, g the gravitational acceleration and Z the geopotential height). MSE is sometimes used as an alternative to the equivalent potential temperature in studies of convection. A high MSE in the boundary layer plays an important role in the development of precipitation (Eltahir, 1998). When the MSE increases, the vertical gradient of MSE between the boundary layer and the free atmosphere also increases, favouring unstable conditions which can trigger precipitation. Furthermore, horizontal gradients of MSE at a range of scales induce thermally direct circulations which redistribute energy towards a flatter horizontal distribution of MSE.

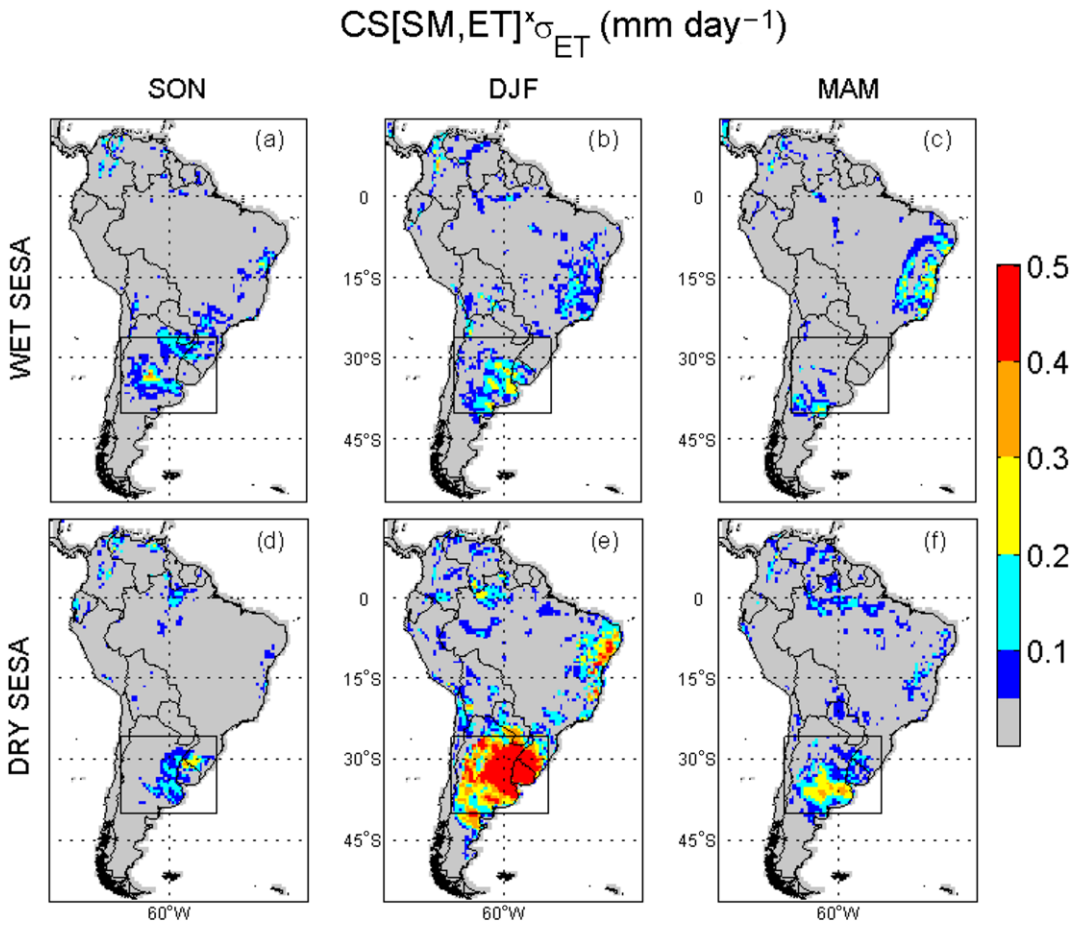

Figure 1. The product between the coupling strength of evapotranspiration (CS[SM,ET]) and its daily variability (σ_{ET}) in South America, for the three austral seasons: spring (SON), summer (DJF) and autumn (MAM) with wet (a–c) and dry (d–f) soil conditions in southeastern South America (inside rectangle).

Previous studies over subtropical South America support the statement that low level circulation and precipitation are sensitive to enhanced soil moisture/surface temperature gradients (Saulo *et al.*, 2010 and references therein).

Over large regions where the horizontal heat advection is small compared with the vertical heat flux, the MSE of the boundary layer is supplied by the sum of the sensible and latent surface heat fluxes (SHF + LHF). The total heat fluxes (SHF + LHF) directly affect the first two terms on the right hand side of Equation (3) and SHF affects the boundary layer depth (BLD). The soil moisture conditions play an important role in the partitioning of surface fluxes into SHF and LHF, represented by the Bowen ratio (BR = SHF/LHF). For example, in the case of dry soils, the BR, SHF and surface temperatures are higher than for wet conditions, resulting in an increase of BLD. However, the sum SHF + LHF does not have such a direct connection with soil moisture as BR has, as SHF + LHF depends on the surface net radiation which is also dependent on cloud cover (Findell and Eltahir, 1999).

In Figure 4, the coupling strength between soil moisture and the variables of Figure 3 for the dry DJF season are shown for SESA. It can be seen that soil moisture is highly coupled to the BR and to the BLD in the entire SESA (Figure 4(a) and (b)). It should be noted that the coupling strength between the consecutive variables in Figure 3 have not been calculated, and that for example high CS[SM,BLD] is interpreted as a result of high CS[SM,BR] through increased/decreased temperatures for dry/wet surface anomalies. The CS[SM,SHF + LHF] (Figure 4(c)) hot spot, however, does not cover the whole SESA but is concentrated over the eastern SESA, consistent with the hypothesis that the relationship between SM and SHF + LHF is not as direct as the relation SM–BR. The coupling strength of MSE (CS[SM,MSE], Figure 4(d), MSE is here calculated at 925 hPa) also shows its maximum value in the eastern SESA area. The coupling strength of the vertical gradient of MSE (CS[SM,Δ(MSE)/Δz]), Figure 4(e), calculated between 925 and 850 hPa) is quite similar to the coupling strength of the vertical humidity flux (CS[SM,wq]), showing the regions where soil moisture influences on the vertical humidity flux through atmospheric instability. Both patterns are similar to the CS[SM,SHF + LHF] pattern, suggesting that this influence is exerted through the coupling of the fluxes. Figure 4(g) indicates that soil moisture could also affect the local to regional scale circulation, here approximated by sea level pressure (SLP).The CS[SM,SLP] pattern has a maximum over southern

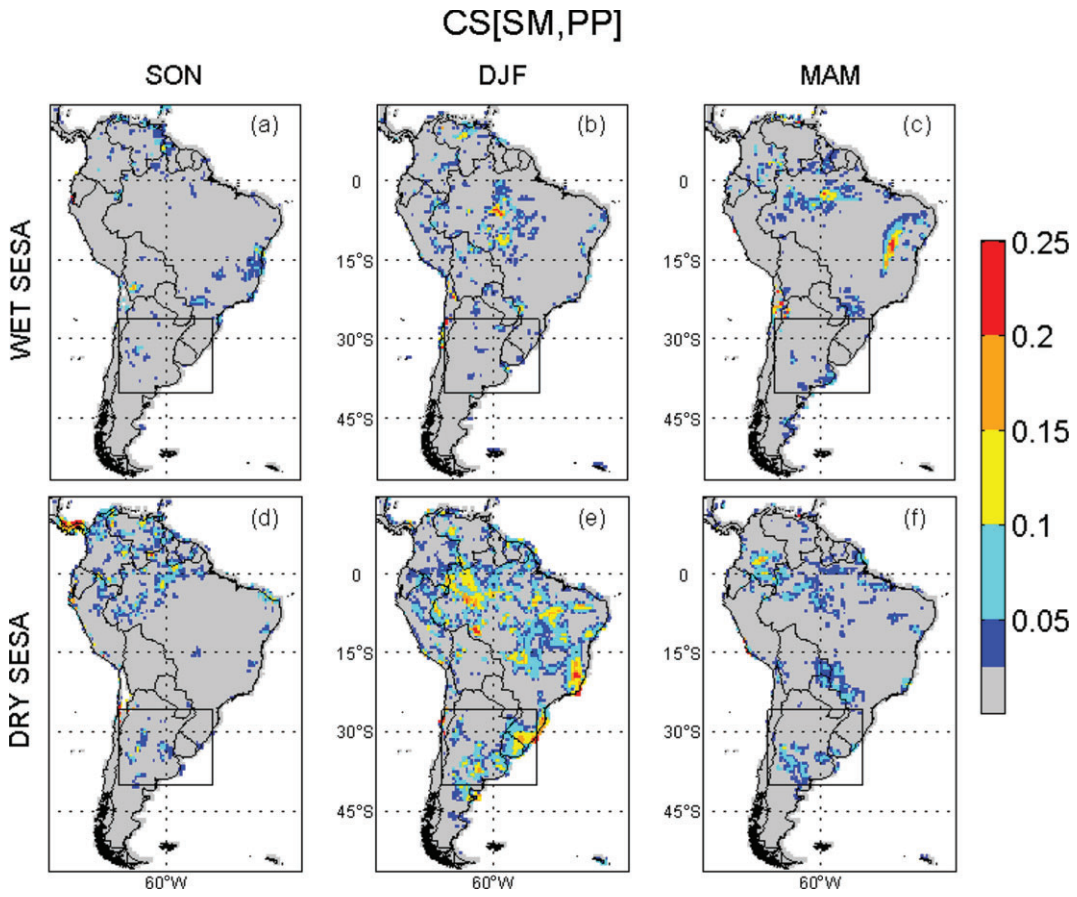

Figure 2. Coupling strength of precipitation (CS[SM,PP]) for the austral seasons: spring (SON), summer (DJF) and autumn (MAM) with wet (a–c) and dry (d–f) soil conditions in southeastern South America (inside rectangle).

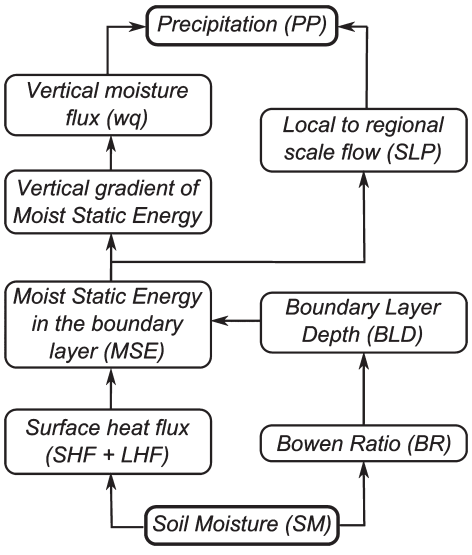

Figure 3. Pathways between soil moisture and precipitation processes (adapted from Eltahir (1998)).

Brazil where the horizontal contrast of CS[SM,MSE] is highest (see Figure 4(d)). Finally, the CS[SM,PP] pattern is shown in Figure 4(h). Considering the analysis of the Figure 4(a)–(g), the hot spot of soil moisture and precipitation coupling over Uruguay and southern Brazil (Figure 2(e)) is probably associated with changes in MSE and in the circulation, induced by soil moisture anomalies.

4. Discussion and conclusions

SESA has a high coupling efficiency when the soil conditions are dry during the summer months. Weaker coupling efficiencies are found in the other seasons and for the wet summer case. This result is a combination of a high variability of the evapotranspiration during summer together with higher soil moisture – evapotranspiration coupling over dry than wet soil conditions. The latter can be understood as a major sensitivity of the evapotranspiration to changes in soil moisture content when the soil is dry, which has already been documented in previous studies (e.g. Wei and Dirmeyer, 2012). With respect to precipitation, high coupling values appear during the same dry DJF period but only over the eastern part of the SESA region. To understand this difference between eastern and western SESA, the coupling between soil moisture and some of the variables that are included in the pathways between soil moisture and precipitation were analysed.

While the couplings of soil moisture with the BR and of soil moisture with the BLD are high over all SESA, the coupling of soil moisture with the surface heat flux

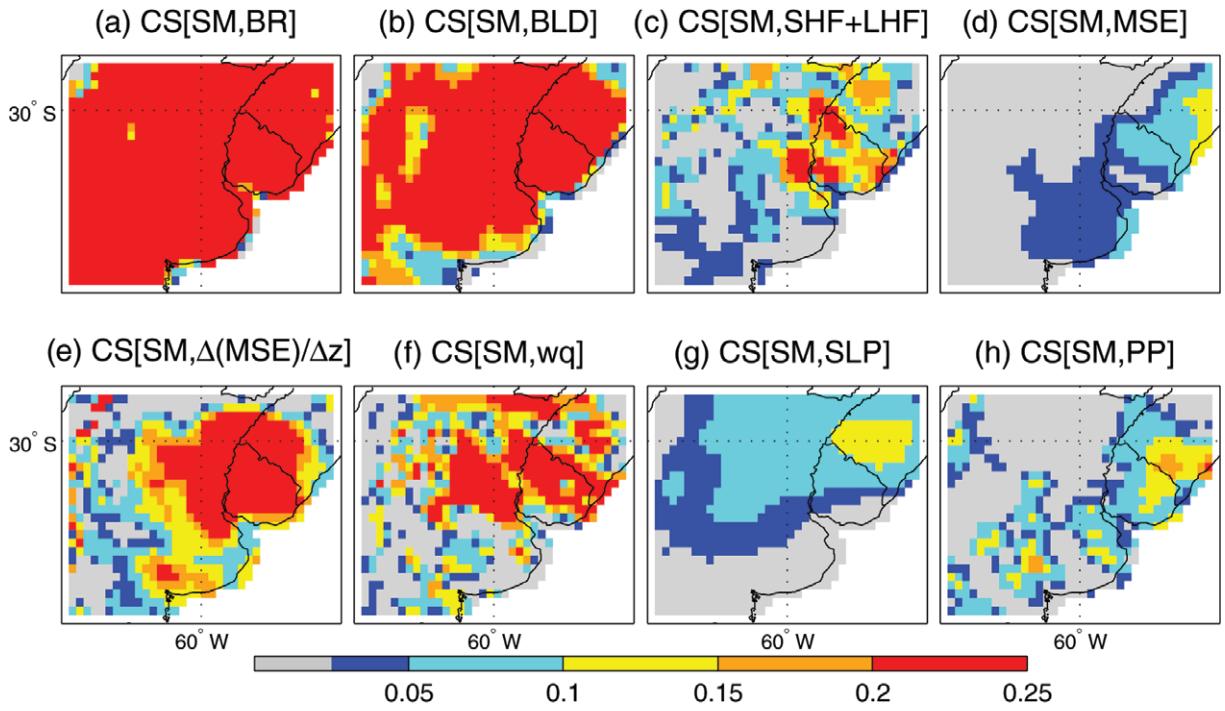

Figure 4. Coupling strength of the variables: (a) Bowen ratio (BR), (b) boundary layer depth (BLD), (c) surface heat flux (SHF + LHF), (d) moist static energy at 925 hPa (MSE), (e) vertical gradient of MSE between 925 and 850 hPa (Δ(MSE)/Δz), (f) vertical humidity flux (wq), (g) sea level pressure (SLP) and (h) precipitation in southeastern South America.

has a hot spot over eastern SESA. This generates coupling between soil moisture and MSE in the boundary layer as well as a higher coupling of soil moisture with the vertical gradient of MSE over eastern SESA. The vertical gradient of MSE seems to affect precipitation through coupling of soil moisture with the vertical moisture flux out of the boundary layer (we assumed that this vertical flow is enhanced in unstable conditions, thus favouring convection). It is also seen that the coupling of soil moisture with MSE is high over Uruguay and southern Brazil near the region of high coupling between soil moisture and SLP, suggesting that in this area soil moisture could affect the circulation in the lower levels of the atmosphere. This leads to the conclusion that precipitation is linked with soil moisture through the MSE in SESA during this dry summer.

The CS index embeds all aspects of the soil moisture field influence on precipitation, such as local water recycling (e.g. Trenberth, 1999), indirect local processes such as atmospheric thermodynamic properties (e.g. Beljaars *et al.*, 1996) and non-local processes such as advection of external moisture into the region (e.g. Spracklen *et al.*, 2012). It is worth mentioning that although a high coupling efficiency is commonly considered to be a necessary condition for a high coupling of precipitation, we find regions where this condition does not apply, such as in central and northern Brazil during the SESA-dry DJF season. This is an indication of non-local impact of soil moisture on precipitation such as advection of moisture from a remote source as suggested by e.g. Goessling and Reick (2011). Wei and Dirmeyer (2012) estimated the remote coupling between soil moisture and precipitation to around 20% of total global coupling and van der Ent and Savenije (2011) found that 70% of the water resources in the SESA region comes from evapotranspiration from the Amazon rainforest.

Contrasting hypothesis about the sign of soil moisture –precipitation coupling, have been presented by different authors. In relation to the vertical gradient of MSE, while Eltahir (1998) suggested a positive influence on precipitation, Cook *et al.* (2006) proposed that an increased in the vertical gradient of MSE would lead to reduced precipitation through higher atmospheric stability. The results presented here are based on the CS index, which does not distinguish between positive and negative influences. The serial correlation between the vertical gradient of MSE and precipitation was calculated for all grid points of SESA where the coupling strength is higher than 0.025. At 83% of these grid points the correlation is positive, indicating that the vertical gradient of MSE influences positively on precipitation. The hot spot of both precipitation and vertical gradient of MSE and the positive correlation between the two variables are evidence for a positive feedback mechanism for eastern SESA during a dry summer.

Acknowledgements

Simulations were made with the high-performance computing clusters available at CIMA/UBA-CONICET, Argentina. We acknowledge the project PIP 112-200801-01788 (CONICET, Argentina). We also thank Patrick Samuelsson, Marco Kupiainen and Gabriel Vieytes for technical support and the anonymous reviewers for their valuable comments on the manuscript.

References

Barreiro M, Díaz N. 2011. Land–atmosphere coupling in El Niño influence over South America. *Atmospheric Science Letters* **12**: 351–355, doi: 10.1002/asl.348.

Beljaars ACM, Viterbo P, Miller MJ, Betts AK. 1996. The anomalous rainfall over the United States during July 1993: sensitivity to land surface parameterization and soil moisture anomalies. *Monthly Weather Review* **124**: 362–383, doi: 10.1175/1520-0493(1996)124<0362:tarotu>2.0.co;2.

Cook BI, Bonan GB, Levis S. 2006. Soil moisture feedbacks to precipitation in Southern Africa. *Journal of Climate* **19**: 4198–4206, doi: 10.1175/JCLI3856.1.

Dee DP et al. 2011. The ERA-Interim reanalysis: configuration and performance of the data assimilation system. *Quarterly Journal of the Royal Meteorological Society* **137**: 553–597, doi: 10.1002/qj.828.

Eltahir EAB. 1998. A soil moisture–rainfall feedback mechanism: 1. Theory and observations. *Water Resources Research* **34**(4): 765–776, doi: 10.1029/97WR03499.

van der Ent RJ, Savenije HHG. 2011. Length and time scales of atmospheric moisture recycling. *Atmospheric Chemistry and Physics* **11**: 1853–1863, doi: 10.5194/acp-11-1853-2011.

Findell KL, Eltahir EAB. 1999. Analysis of the pathways relating soil moisture and subsequent rainfall in Illinois. *Journal of Geophysical Research* **104**(D24): 31565–31574, doi: 10.1029/1999JD900757.

Goessling HF, Reick CH. 2011. What do moisture recycling estimates tell us? Exploring the extreme case of non-evaporating continents. *Hydrology and Earth System Sciences* **15**: 3217–3235, doi: 10.5194/hess-15-3217-2011.

Guo Z, Dirmeyer PA. 2013. Interannual variability of land–atmosphere coupling strength. *Journal of Hydrometeorology* **14**: 1636–1646, doi: 10.1175/JHM-D-12-0171.1.

Guo Z et al. 2006. GLACE: the global land-atmosphere coupling experiment. Part II: Analysis. *Journal of Hydrometeorology* **7**: 611–625, doi: 10.1175/JHM511.1.

Koster RD et al. 2004. Regions of strong coupling between soil moisture and precipitation. *Science* **305**: 1138–1140, doi: 10.1126/science.1100217.

Koster RD et al. 2006. GLACE: the global land-atmosphere coupling experiment. Part I: Overview. *Journal of Hydrometeorology* **7**: 590–610, doi: 10.1175/jhm510.1.

Ma HY, Mechoso CR, Xue Y, Xiao H, Wu CM, Li JL, de Sales F. 2011. Impact of land surface processes on the South American warm season climate. *Climate Dynamics* **37**: 187–203, doi: 10.1007/s00382-010-0813-3.

Masson V, Champeaux JL, Chauvin F, Meriguet C, Lacaze R. 2003. A global database of land surface parameters at 1-km resolution in meteorological and climate models. *Journal of Climate* **16**: 1261–1282, doi: 10.1175/1520-0442-16.9.1261.

Menéndez CG, De Castro M, Sörensson AA, Boulanger JP. 2010. CLARIS project: towards climate downscaling in South America. *Meteorologische Zeitschrift* **19**: 357–362, doi: 10.1127/0941-2948/2010/0459.

Ruscica RC, Sörensson AA, Menéndez CG. 2014. Hydrological links in Southeastern South America: soil moisture memory and coupling within a hot spot. *International Journal of Climatology* **34**: 3641–3653, doi: 10.1002/joc.3930.

Samuelsson P et al. 2011. The Rossby Centre Regional Climate model RCA3: model description and performance. *Tellus Series A: Dynamic Meteorology and Oceanography* **63**: 4–23, doi: 10.1111/j.1600-0870.2010.00478.x.

Santanello JA, Peters-Lidard CD, Kumar SV. 2011. Diagnosing the sensitivity of local land–atmosphere coupling via the soil moisture–boundary layer interaction. *Journal of Hydrometeorology* **12**: 766–786, doi: 10.1175/JHM-D-10-05014.1.

Saulo C, Ferreira L, Nogués-Paegle J, Seluchi M, Ruiz J. 2010. Land atmosphere interactions during a northwestern Argentina low event. *Monthly Weather Review* **138**: 2481–2498, doi: 10.1175/2010mwr3227.1.

Seneviratne SI, Lüthi D, Litschi M, Schär C. 2006. Land–atmosphere coupling and climate change in Europe. *Nature* **443**: 205–209, doi: 10.1038/nature05095.

Solman S et al. 2013. Evaluation of an ensemble of regional climate model simulations over South America driven by the ERA-Interim reanalysis: model performance and uncertainties. *Climate Dynamics* **41**: 1139–1157, doi: 10.1007/s00382-013-1667-2.

Sörensson AA, Menéndez CG. 2011. Summer soil-precipitation coupling in South America. *Tellus Series A: Dynamic Meteorology and Oceanography* **63**: 56–68, doi: 10.1111/j.1600-0870.2010.00468.x.

Spracklen DV, Arnold SR, Taylor CM. 2012. Observations of increased tropical rainfall preceded by air passage over forests. *Nature* **489**: 282–285, doi: 10.1038/nature11390.

Trenberth KE. 1999. Atmospheric moisture recycling: role of advection and local evaporation. *Journal of Climate* **12**: 1368–1381, doi: 10.1175/1520-0442(1999)012<1368:AMRROA>2.0.CO;2.

Wei J, Dirmeyer PA. 2012. Dissecting soil moisture-precipitation coupling. *Geophysical Research Letters* **39**: L19711, doi: 10.1029/2012GL053038.

Yamada TJ, Koster RD, Kanae S, Oki T. 2007. Estimation of predictability with a newly derived index to quantify similarity among ensemble members. *Monthly Weather Review* **135**(7): 2674–2687, doi: 10.1175/MWR3418.

